Electronic Supplementary Material (ESI) for Chemical Science.


# Surface chemistry dictates stability and oxidation state of supported single metal catalyst atoms

Konstantinos Alexopoulos and Dionisios G. Vlachos*

*Department of Chemical and Biomolecular Engineering and Catalysis Center for Energy Innovation, University of Delaware, 221 Academy St., Newark, DE 19716, USA*

* Corresponding author: vlachos@udel.edu

## Oxygen adsorption energy and diffusion of single metal atoms

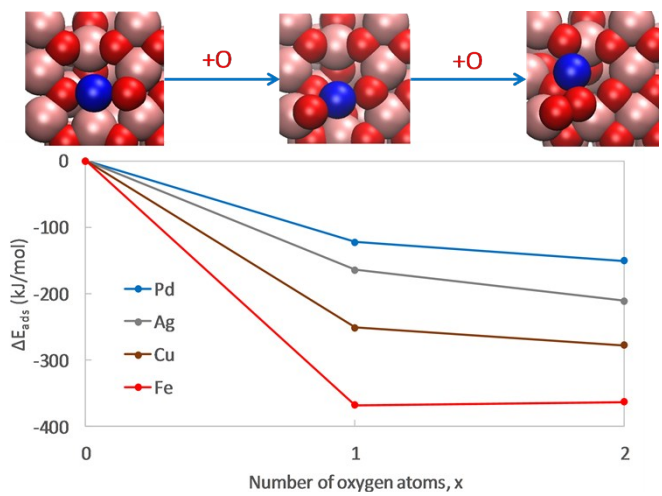


***Fig. S1.*** *Oxygen adsorption energy,* $\Delta E_{ads} = E_{M_1O_x/Al_2O_3} - E_{M_1/Al_2O_3} - 0.5xE_{O_{2(g)}}$, *on alumina-supported single metal (M) atoms as a function of oxygen atoms added (color code: red, O; pink, Al; blue, Pd).*

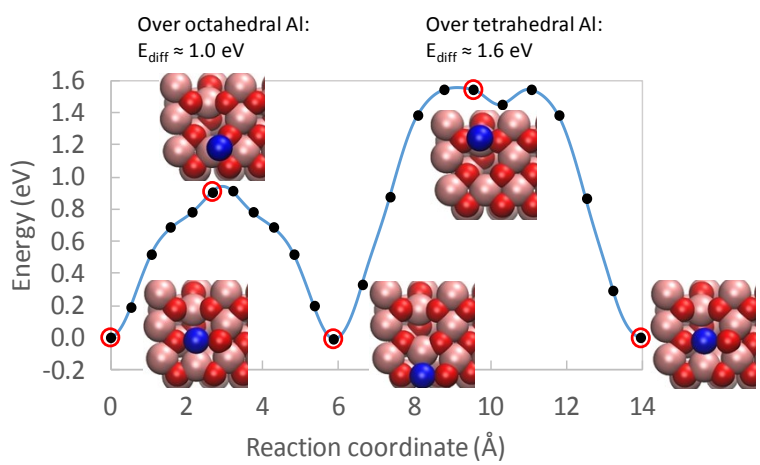


***Fig. S2.*** *Reaction coordinate for diffusion of a single Pd atom on alumina. Color code: red, O; pink, Al; blue, Pd.*

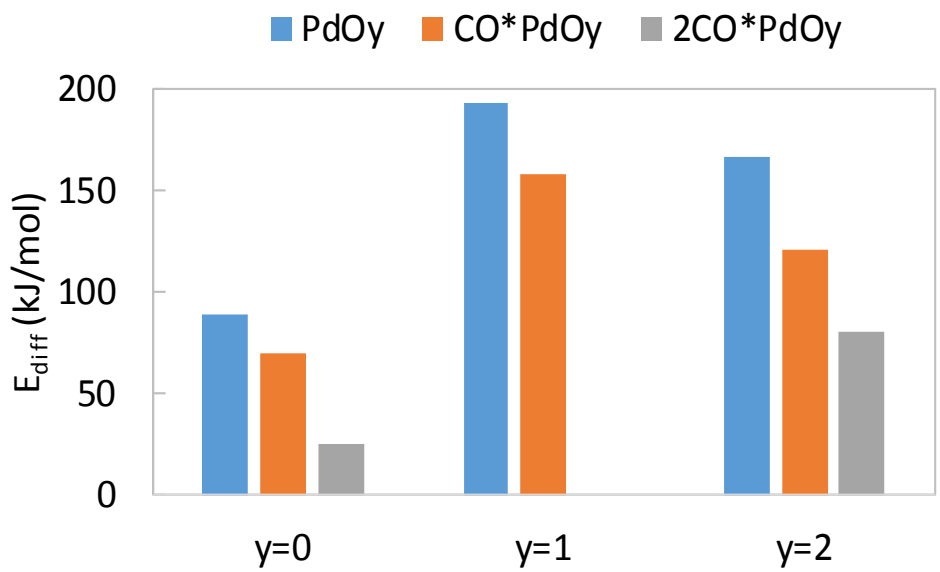


***Fig. S3.*** *Diffusion barriers of isolated $(CO)_xPdO_y$ species (with x, y = 0, 1, 2) over octahedral Al atoms on alumina.*

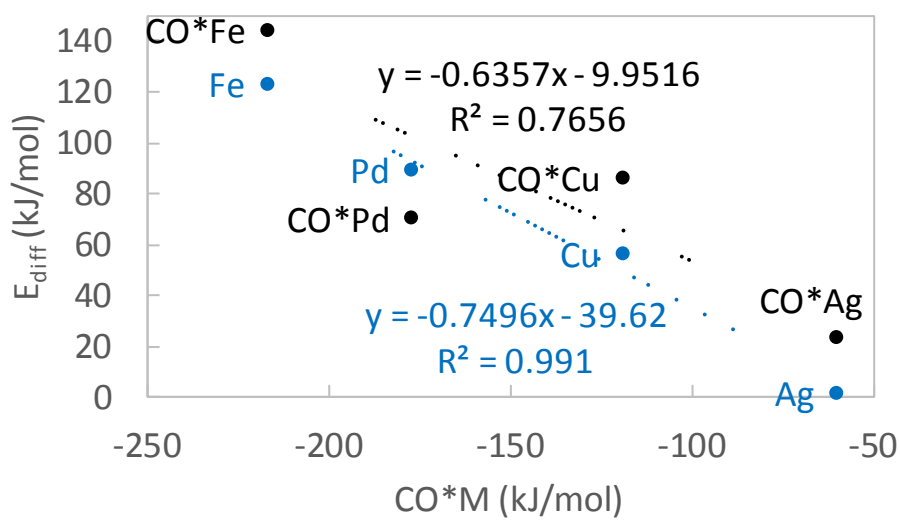


***Fig. S4.*** *Activation energy for the diffusion of CO*M and M species (M = Fe, Pd, Cu, Ag) on alumina as a function of CO adsorption energy on M.*

## Full microkinetic model for CO oxidation on adsorbed single metal atoms

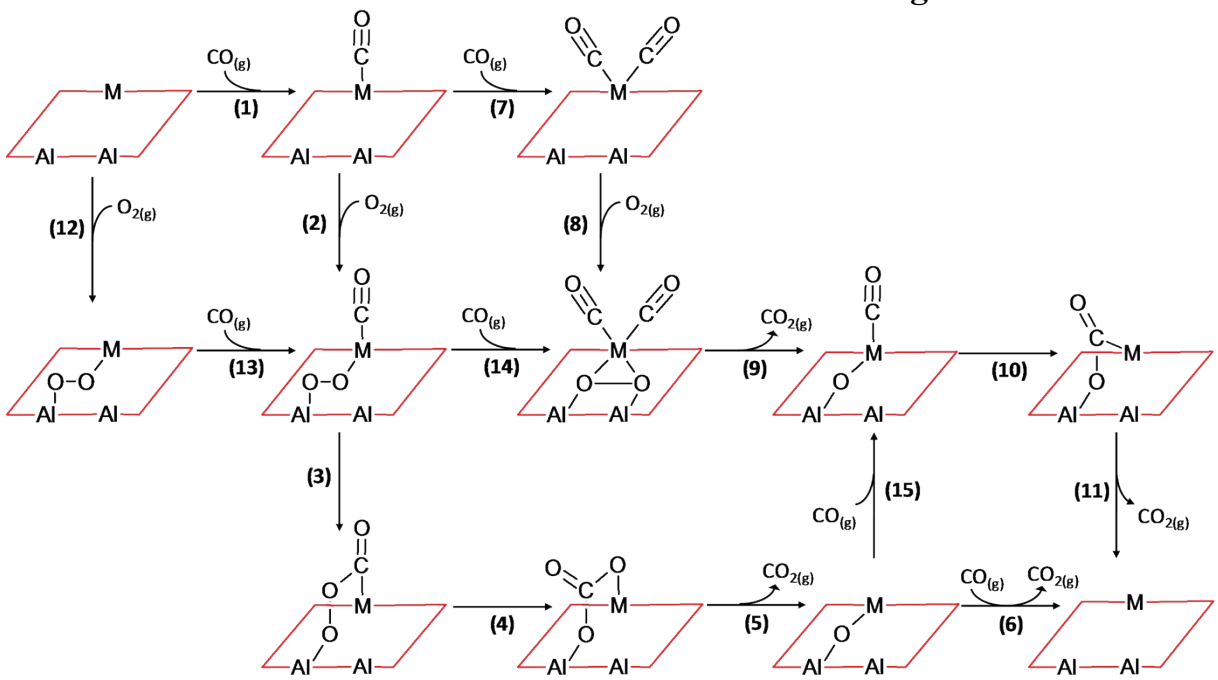


***Fig. S5.*** *Reaction network of CO oxidation over single metal (M) atoms supported on alumina (adapted with permission from ref. 1).*

***Table S1.*** *Kinetic parameters for CO oxidation over adsorbed single metal atoms. Arrhenius activation energies ($E_a$, kJ/mol) and pre-exponential factors (A) as obtained by regression of the ab initio calculated rate coefficients in the temperature range of 300–800 K (see ref. 2 for more details on how the ab initio rate coefficients are calculated and regressed). The standard state for all gas-phase references (i.e., CO, $O_2$, $CO_2$) is taken as p° = 1 bar.*

| Elementary step as per Fig. S5 | $Pd_1/Al_2O_3$[a] | | | | $Fe_1/Al_2O_3$ | | | |
|---|---|---|---|---|---|---|---|---|
| | Forward | | Reverse | | Forward | | Reverse | |
| | $E_a$ | A | $E_a$ | A | $E_a$ | A | $E_a$ | A |
| (1) | 4 | $2.8\ 10^{13}$ | 164 | $1.2\ 10^{21}$ | 4 | $2.8\ 10^{13}$ | 204 | $8.0\ 10^{20}$ |
| (2) | 4 | $2.8\ 10^{13}$ | 41 | $1.8\ 10^{21}$ | 4 | $2.8\ 10^{13}$ | 215 | $1.9\ 10^{22}$ |
| (3) | 79 | $6.3\ 10^{11}$ | 107 | $1.5\ 10^{13}$ | 138 | $2.2\ 10^{13}$ | 50 | $3.1\ 10^{13}$ |
| (4) | 28 | $1.9\ 10^{13}$ | 307 | $4.1\ 10^{13}$ | 23 | $1.6\ 10^{13}$ | 409 | $3.6\ 10^{13}$ |
| (5) | 110 | $3.8\ 10^{21}$ | 4 | $2.8\ 10^{13}$ | 70 | $2.8\ 10^{21}$ | 4 | $2.8\ 10^{13}$ |
| (6) | 0 | $3.3\ 10^{6}$ | 169 | $3.0\ 10^{6}$ | 75 | $2.6\ 10^{6}$ | 0 | $3.7\ 10^{6}$ |
| (7) | 4 | $2.8\ 10^{13}$ | 59 | $1.6\ 10^{20}$ | 4 | $2.8\ 10^{13}$ | 107 | $5.4\ 10^{20}$ |
| (8) | 4 | $2.8\ 10^{13}$ | 85 | $8.7\ 10^{22}$ | 4 | $2.8\ 10^{13}$ | 201 | $5.8\ 10^{22}$ |
| (9) | 131 | $9.9\ 10^{12}$ | 372 | $7.4\ 10^{5}$ | 19 | $4.7\ 10^{13}$ | 215 | $3.0\ 10^{6}$ |
| (10) | 84 | $1.4\ 10^{13}$ | 178 | $5.6\ 10^{13}$ | 95 | $5.8\ 10^{13}$ | 78 | $2.5\ 10^{14}$ |
| (11) | 69 | $7.3\ 10^{21}$ | 4 | $2.8\ 10^{13}$ | 118 | $9.9\ 10^{21}$ | 4 | $2.8\ 10^{13}$ |
| (12) | 4 | $2.8\ 10^{13}$ | 139 | $3.1\ 10^{22}$ | 4 | $2.8\ 10^{13}$ | 331 | $1.3\ 10^{21}$ |
| (13) | 4 | $2.8\ 10^{13}$ | 66 | $7.0\ 10^{19}$ | 4 | $2.8\ 10^{13}$ | 89 | $1.2\ 10^{22}$ |
| (14) | 4 | $2.8\ 10^{13}$ | 103 | $7.9\ 10^{21}$ | 4 | $2.8\ 10^{13}$ | 93 | $1.7\ 10^{21}$ |
| (15) | 4 | $2.8\ 10^{13}$ | 144 | $1.6\ 10^{21}$ | 4 | $2.8\ 10^{13}$ | 58 | $3.2\ 10^{21}$ |

[a] Reproduced with permission from ref. 1.

## Validation of analytical rate expressions

To ensure that the analytical rate equations (see main text) are accurate for both Pd- and Fe-based single atom catalysts, these rate expressions were validated against the full microkinetic model for CO oxidation (Table S1). As illustrated in Fig. S6, the agreement with the full model in terms of TOFs and coverages is excellent.

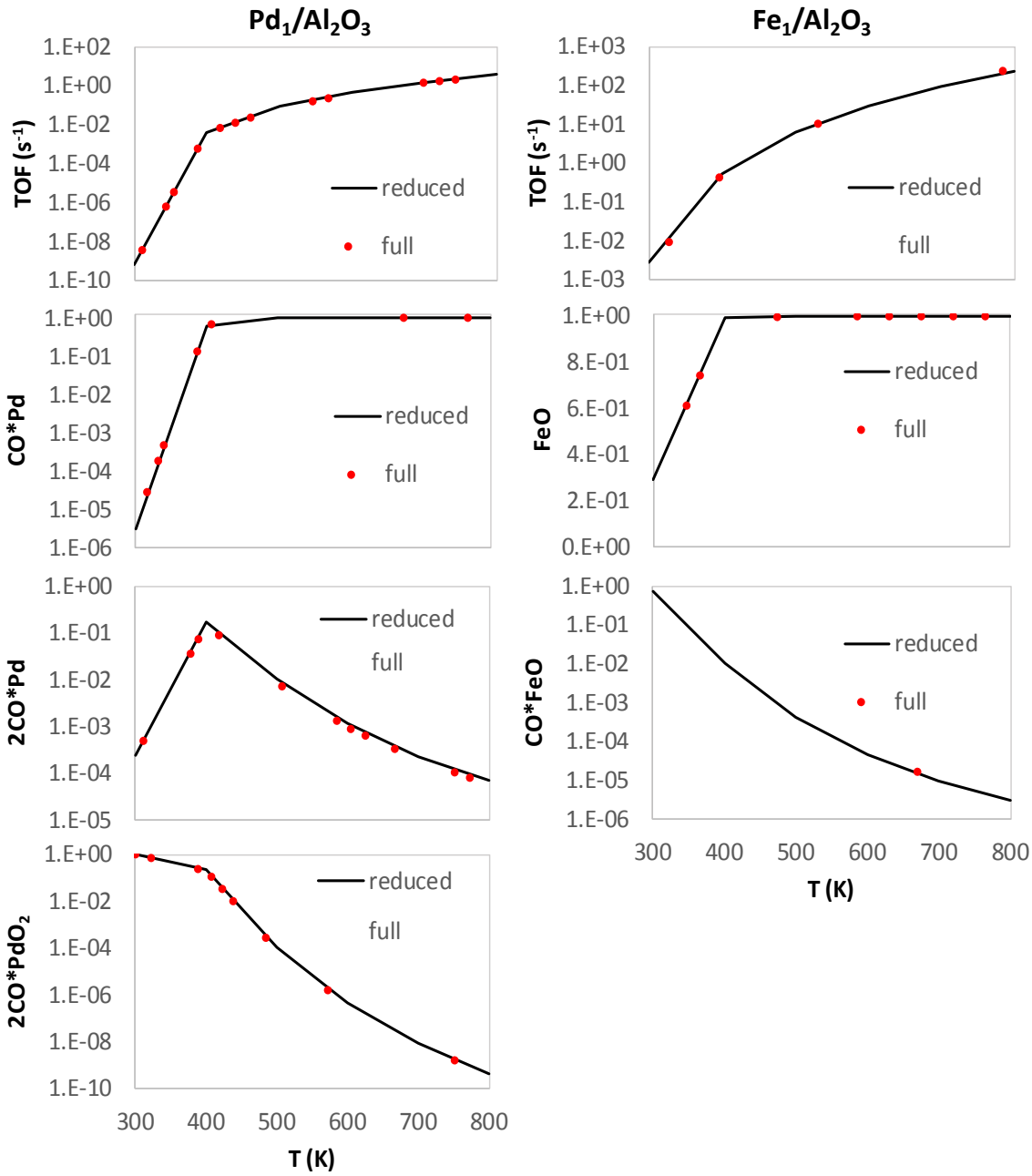


***Fig. S6.*** *Simulated turnover frequencies (TOF) and surface coverages for CO oxidation on* $Pd_1/Al_2O_3$ *and* $Fe_1/Al_2O_3$ *using the full microkinetic model of Table S1 vs. the analytical rate expressions of the main text;* $p_{CO} = p_{O2} = 0.1$ *bar.*

## Effect of $CO_2$ on surface coverages

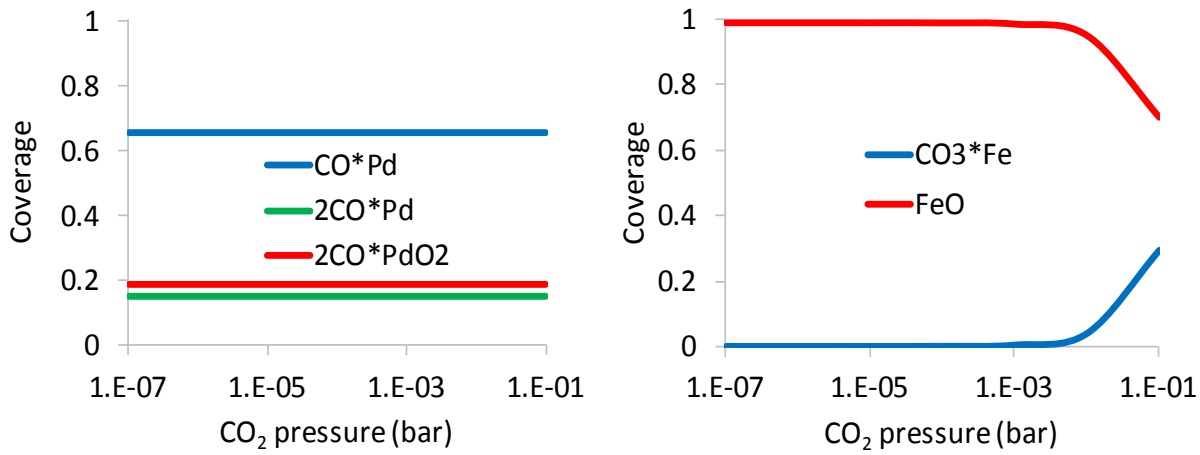


***Fig. S7.*** *Surface coverages for CO oxidation on $Pd_1/Al_2O_3$ and $Fe_1/Al_2O_3$ in the presence of $CO_2$; T = 400 K, $p_{CO} = p_{O2} = 0.1$ bar. The full microkinetic model of Table S1 is used for these simulations.*

## Tracking the formal oxidation state of the active site on single atom catalysts

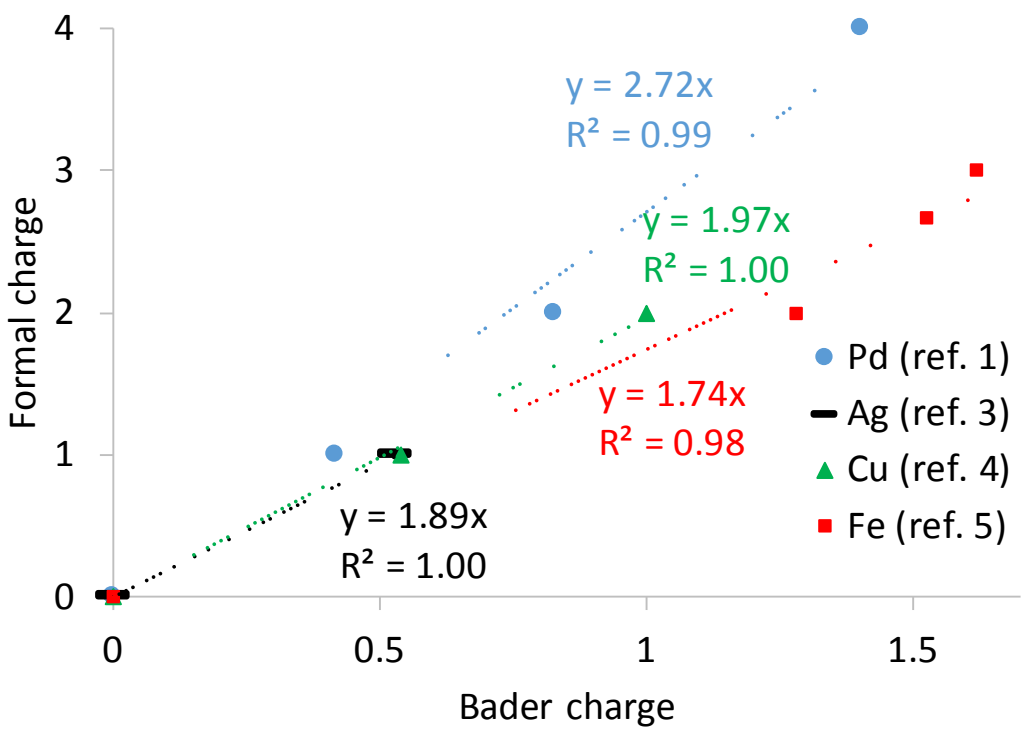


***Fig. S8.*** *Calibration of Bader charges to obtain the formal charges on different elements.*

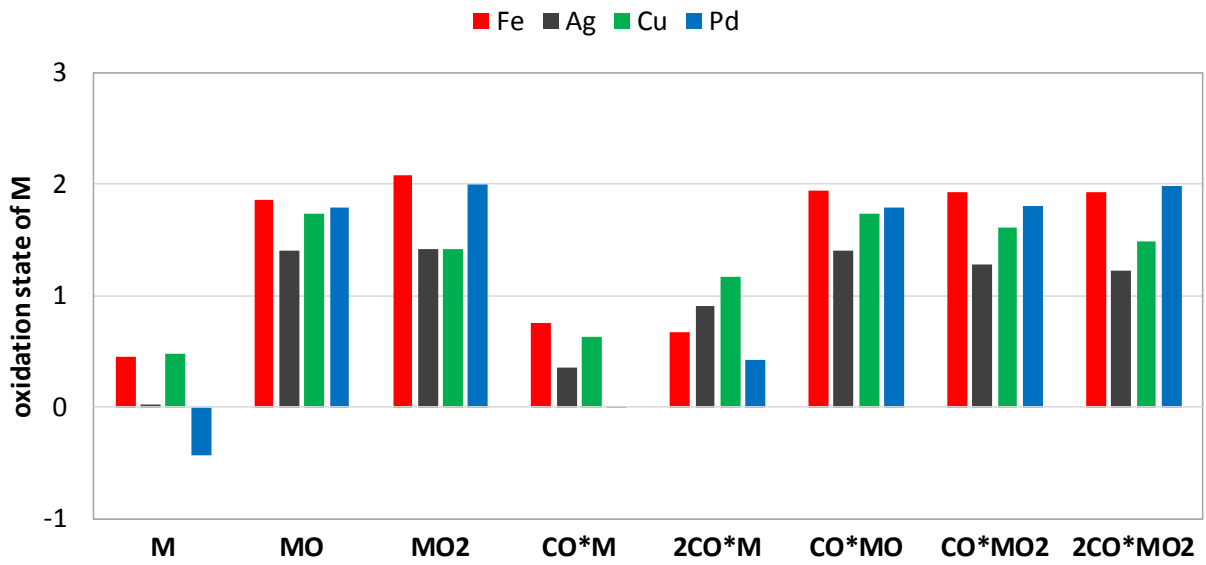


***Fig. S9.*** *Element-specific oxidation state of different single metal atom species. Since the oxidation state varies when changing the element, the oxidation state for a generic M element with composition* $(CO)_xMO_y$ *(x=0, 1, 2; y=0, 1, 2) is taken as the average of the corresponding species over the investigated elements (Pd, Cu, Ag, and Fe).*

***Table S2.*** *Average oxidation state with its 95% confidence interval for the different single metal atom species (as per Fig. S9).*

| | |
|---|---|
| M | 0.1 ± 0.4 |
| MO | 1.7 ± 0.2 |
| MO2 | 1.7 ± 0.3 |
| CO*M | 0.4 ± 0.3 |
| 2CO*M | 0.8 ± 0.3 |
| CO*MO | 1.7 ± 0.2 |
| CO*MO2 | 1.7 ± 0.2 |
| 2CO*MO2 | 1.7 ± 0.3 |

## Principal component analysis on adsorbed single metal atoms

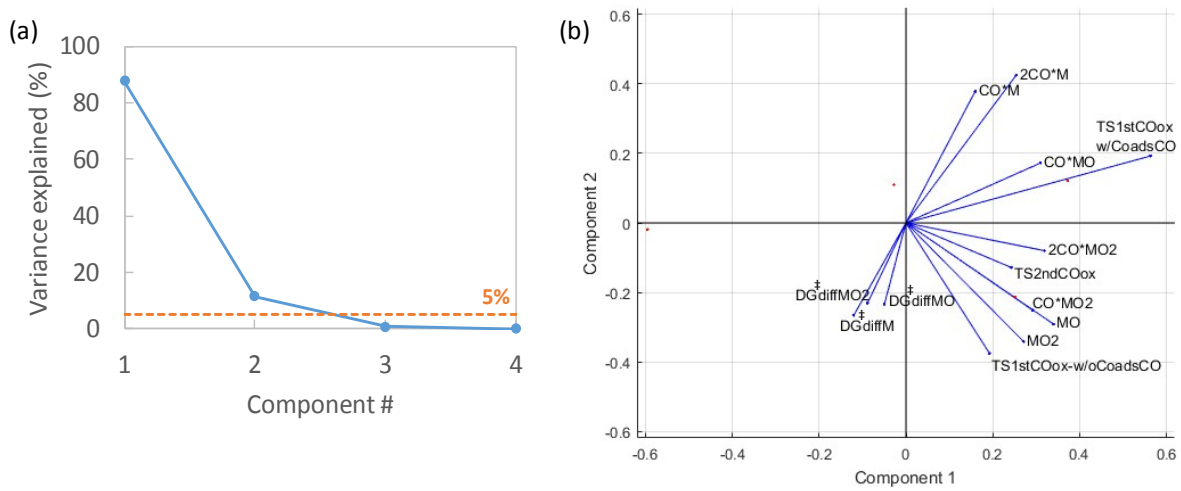


***Fig. S10.*** *(a) Scree plot showing that two components are needed in order to describe most of the variance in the dataset. (b) Biplot graph showing that the two descriptors used in the present study (namely the CO*M and MO2 free energies) are indeed orthogonal to each other.* $DG^{\ddagger}_{diffMOy}$ *(y=0,1,2) is almost collinear with the free energy of CO*M, justifying its use as the sole descriptor for the diffusion barrier.*

## Boundaries between different rate-determing step (RDS) regions

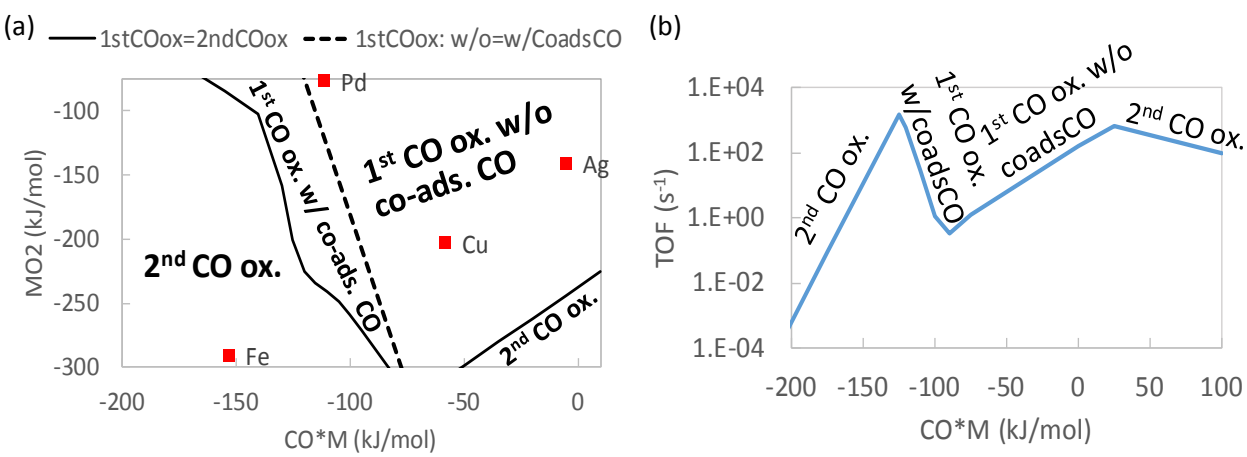


***Fig. S11.*** *(a) Boundary lines separating regions controlled by different RDSs;* $p_{CO} = p_{O2} = 0.1$ *bar, T = 400 K. Boundary lines defined as:* $TOF_{1stCOox} = TOF_{2ndCOox}$ *at the full line,* $TOF_{1stCOox\text{-}w/CoadsCO} = TOF_{1stCOox\text{-}w/oCoadsCO}$ *at the dashed line. A root-finding method is used to construct these boundary lines based on the analytical rate expressions developed in the main text. (b) Overall TOF for the same (T, p) conditions and at a fixed MO2 free energy of -210 kJ/mol, with the different slopes as a function of CO*M free energy corresponding to different dominant RDS.*

## References


1. K. Alexopoulos, Y. Wang and D. G. Vlachos, *ACS Catal.*, 2019, **9**, 5002.
2. M. John, K. Alexopoulos, M.-F. Reyniers and G. B. Marin, *ACS Catal.*, 2016, **6**, 4081.
3. P. T. Chen, E. C. Tyo, M. Hayashi, M. J. Pellin, O. Safonova, M. Nachtegaal, J. A. van Bokhoven, S. Vajda and P. Zapol, *J. Phys. Chem. C*, 2017, **121**, 6614.
4. S. K. Iyemperumal and N. A. Deskins, *Phys. Chem. Chem. Phys.*, 2017, **19**, 28788.
5. Y. Meng, X. W. Liu, C. F. Huo, W. P. Guo, D. B. Cao, Q. Peng, A. Dearden, X. Gonze, Y. Yang, J. Wang and H. Jiao, *J. Chem. Theory Comput.*, 2016, **12**, 5132.